M. Staat, J. Ballmann: Fundamental Aspects of Numerical Methods for the Propagation of Multidimensional Nonlinear Waves in Solids. In J. Ballmann, R. Jeltsch (Eds.): *Nonlinear Hyperbolic Equations - Theory, Computation Methods, and Applications*. Vieweg, Braunschweig/Wiesbanden (1989) 574-588.
http://opus.bibliothek.fh-aachen.de/opus/volltexte/2007/206/

FUNDAMENTAL ASPECTS OF NUMERICAL METHODS FOR THE PROPAGATION OF MULTI-DIMENSIONAL NONLINEAR WAVES IN SOLIDS

M. Staat, J. Ballmann
Lehr- und Forschungsgebiet Mechanik
RWTH Aachen
D - 5100 Aachen, FRG

SUMMARY

The nonlinear scalar constitutive equations of gases lead to a change in sound speed from point to point as would be found in linear inhomogeneous (and time dependent) media. The nonlinear tensor constitutive equations of solids introduce the additional local effect of solution dependent anisotropy. The speed of a wave passing through a point changes with propagation direction and its rays are inclined to the front. It is an open question whether the widely used operator splitting techniques achieve a dimensional splitting with physically reasonable results for these multi-dimensional problems.

Maybe this is the main reason why the theoretical and numerical investigations of multi-dimensional wave propagation in nonlinear solids are so far behind gas dynamics. We hope to promote the subject a little by a discussion of some fundamental aspects of the solution of the equations of nonlinear elastodynamics. We use methods of characteristics because they only integrate mathematically exact equations which have a direct physical interpretation.

INTRODUCTION

Many characteristic-based methods have been devised for the solution of hyperbolic problems with more than two independent variables (e.g. two- and three-dimensional wave propagation). Most of them (e.g. GODUNOV-Type-Methods and GLIMM's Random-Choice-Method) use schemes developed for one-dimensional wave propagation by various operator splitting techniques. Maybe this is the reason, why promising results are only known for nonlinear media with scalar constitutive equations so far.

The mechanical state variables for solids are second order tensors, and thus only physically one-dimensional problems can be modelled by scalar laws, whereas tensor constitutive equations describe the material behaviour in multi-dimensional problems. Thereby a strong coupling of the different spatial directions may result and, if the material is nonlinear, local effects of anisotropy may occur. Such effects are probably best known from magnetohydrodynamics

and from optical and mechanical waves in linear anisotropic solids [1, 2]. Due to the dependence on the solution, the situation is even more complicated for nonlinear elastic and plastic waves in solids. A scalar nonlinear constitutive equation introduces a solution dependent inhomogeneity. Nonlinear tensor constitutive equations cause the additional local effect of solution dependent anisotropy.

For a numerical treatment of these nonlinear problems, methods of nearcharacteristics have been devised. which become methods of bicharacteristics, if the local scheme uses the axes of symmetry of the local wave fronts of point disturbances [3, 4]. The complete set of PDE's describing a general nonlinear elastic solid can be solved numerically for arbitrary large deformations and large displacements. For convenience we restrict our discussion to hyperelastic materials. One can easily dispense with the lengthier treatment of CAUCHYelastic materials as included in [4], since in a purely mechanical theory every stable passive elastic material is hyperelastic (or GREEN-elastic) [5]. Furthermore we exclude all physical situations for incompressible solids that do not permit longitudinal waves, e.g. plain strain problems but not plain stress problems.

BASIC EQUATIONS

The material points of a body are denoted by their coordinates in a possible reference configuration $\bar{B}^*$ and the actual configuration B^* in space and time by point-coordinates ξ^a and x^a $(a = 0, 1, 2, 3)$, respectively. The time-like coordinates are $\xi^0 = c\tau$ and $x^0 = ct$ with time $\tau = t$, and some constant speed c. Co-and contravariant basis vectors are introduced in both configurations in the usual manner. The material points with position vector $\bar{\mathbf{r}}^* = \xi^0 \bar{\mathbf{g}}_{\bar{0}} + \bar{\mathbf{r}}$ in $\bar{B}^*$ are moved by a displacement field $\mathbf{u}(\bar{\mathbf{r}}^*)$ into their position $\mathbf{r}^* = x^0 \mathbf{g}_0 + \mathbf{r}$ with $\mathbf{r} = \bar{\mathbf{r}} + \mathbf{u}$. The dyadic notation of the material displacement of a field $f(\bar{\mathbf{r}}^*)$ over $\bar{B}^*$ is given by

$$\bar{\nabla}^* f := \frac{1}{c}\frac{\partial f}{\partial \tau} \circ \bar{\mathbf{g}}^{\bar{0}} + \bar{\nabla} f =: \frac{\partial f}{\partial \xi^\alpha} \circ \bar{\mathbf{g}}^{\bar{\alpha}}, \quad (\alpha = 0, 1, 2, 3), \tag{1}$$

The local approximation of the bijective mapping in space $x^i(\xi^0, \xi^1, \xi^2, \xi^3)$, $i = 1, 2, 3$ is the deformation gradient

$$\bar{\mathbf{F}} := \bar{\nabla}\mathbf{r}. \tag{2}$$

Other useful kinematic tensors are the displacement derivative $\bar{\mathbf{H}}$, the positive definite right CAUCHY-GREEN-tensor $\mathbf{C}$ or the GREEN-deformation tensor $\mathbf{G}$. With the purely space-like unit dyadic $\mathbf{E}$ we have

$$\bar{\mathbf{H}} := \bar{\nabla}\mathbf{u} = \bar{\mathbf{F}} - \mathbf{E}, \quad \delta\bar{\mathbf{H}} = \delta\bar{\mathbf{F}}, \tag{3a}$$

$$\mathbf{C} := \bar{\mathbf{F}}^{\mathrm{T}}\bar{\mathbf{F}}, \quad \mathbf{C}^{\mathrm{T}} = \mathbf{C}, \quad \mathrm{III} := \det \mathbf{C} = \det^2 \bar{\mathbf{F}} \neq 0, \tag{3b}$$

$$\mathbf{G} := \frac{1}{2}(\mathbf{C} - \mathbf{E}) = \frac{1}{2}\left(\bar{\mathbf{H}} + \bar{\mathbf{H}}^{\mathrm{T}} + \bar{\mathbf{H}}^{\mathrm{T}}\bar{\mathbf{H}}\right). \tag{3c}$$

To any of these deformation tensors, there is a conjugate stress tensor which is a single valued tensor function of the deformation for elastic media. For hyperelastic materials the simultaneous invariant of the pairs of conjugate tensors is the stored energy density.

For an elastic material the stress tensor is a single valued function of $\mathbf{C}$ and thus also a deformation measure. This makes the theory of elasticity mathematically attractive, although in the nonlinear theory there is no analytical presentation for the inverse function, [6]. For an isotropic elastic solid the second PIOLA-KIRCHHOFF-stress $\bar{\bar{\boldsymbol{\sigma}}}$ is an isotropic tensor function of $\mathbf{C}$. In three space dimensions we use the following presentations for compressible or incompressible solids, respectively:

$$\bar{\bar{\boldsymbol{\sigma}}}(\mathbf{G}) = \varphi_0'\mathbf{E} + \varphi_1'\mathbf{G} + \varphi_2'\mathbf{G}^2, \tag{4a}$$

$$\bar{\bar{\boldsymbol{\sigma}}}(\mathbf{C}) = \psi_0'\mathbf{E} + \psi_1'\mathbf{C} - p\mathbf{C}^{-1}. \tag{4b}$$

Here φ_0', φ_1', φ_2' and ψ_0', ψ_1' are scalar functions of the invariants of $\mathbf{G}$ and $\mathbf{C}$, respectively. Note, for an incompressible solid only the deviatoric stress is determined from the deformation in three dimensions, since $\mathrm{III} = 1$. In this case the hydrostatic pressure p can be calculated as the solution of a boundary value problem. Furthermore, the incompressible solid allows no longitudinal waves in three dimensions. We therefore exclude this special case from our discussion. For the plane stress problem of a plate one can calculate $p(\mathrm{I}, \mathrm{II})$ - where I, II are principal invariants of $\mathbf{C}$ - and thus obtain for the compressible and incompressible solid the formally similar representations

$$\bar{\bar{\boldsymbol{\sigma}}}(\mathbf{G}) = \varphi_0\mathbf{E} + \varphi_1\mathbf{G}, \tag{4c}$$

$$\bar{\bar{\boldsymbol{\sigma}}}(\mathbf{C}) = \psi_0\mathbf{E} + \psi_1\mathbf{C}. \tag{4d}$$

It is understood that now $\bar{\bar{\boldsymbol{\sigma}}}$, $\mathbf{G}$, $\mathbf{C}$ are tensors in two-dimensional space. The one-dimensional stress $\bar{\bar{\boldsymbol{\sigma}}} := \sigma \bar{\mathbf{g}}_{\bar{1}} \circ \bar{\mathbf{g}}_{\bar{1}}$ may be calculated from a scalar law $\sigma = f(\varepsilon)$ with $\varepsilon := \bar{\mathbf{g}}_{\bar{1}}\mathbf{G}\bar{\mathbf{g}}_{\bar{1}}$. But $\mathbf{G}$ is still three-dimensional (with cylindrical symmetry). Only the trivial hydrostatic stress reduces the constitutive equation to a scalar law, where both $\bar{\bar{\boldsymbol{\sigma}}}$ and $\mathbf{G}$ are spherical tensors. There are longitudinal waves in an incompressible plate, due to the variation of its thickness. Therefore we exclude plane strain for those materials. In the local balance of momentum, written in the reference configuration (multiple dots denote multiple transvection),

$$\bar{\rho} c\left(\bar{\nabla}^* \mathbf{v}\right)\mathbf{E} - \left(\bar{\nabla}^* \bar{\boldsymbol{\sigma}}\right) : \mathbf{E} - \bar{\rho}\mathbf{b} = \mathbf{0}, \tag{5}$$

appears the first PIOLA-KIRCHHOFF-stress $\bar{\boldsymbol{\sigma}}$,

$$\bar{\boldsymbol{\sigma}} := \bar{\mathbf{F}}\bar{\bar{\boldsymbol{\sigma}}}, \quad \bar{\boldsymbol{\sigma}}\,\bar{\mathbf{F}}^{\mathrm{T}} = \bar{\mathbf{F}}\bar{\boldsymbol{\sigma}}^{\mathrm{T}}, \tag{6}$$

which is a single valued tensor function of $\bar{\mathbf{F}}$ by eqs. (3), (4). $\mathbf{v}$, $\bar{\rho}$, $\mathbf{b}$ are the particle velocity, the mass density in the reference configuration and the density of body force, respectively. The material is called hyperelastic if the stress function can be derived from a stored energy density U. This imposes some integrability conditions upon eq. (4). With the fourth order stiffness $\mathbf{A}\left(\bar{\mathbf{F}}\right)$, the constitutive equations may be written in the form

$$\delta\bar{\boldsymbol{\sigma}} = \mathbf{A} : \delta\bar{\mathbf{F}}\,, \tag{7a}$$

where $\mathbf{A}$ can be derived from U for hyperelastic solids:

$$\delta\bar{\mathbf{F}} : \mathbf{A} : \delta\bar{\mathbf{F}} = \bar{\rho}\delta^2 U\,. \tag{7b}$$

From eqs. (3a), (5) and (7a) we have the final balance of momentum

$$\mathbf{l} = \mathbf{0}, \quad \mathbf{l} := \bar{\rho}c\left(\bar{\nabla}^{*}\mathbf{v}\right)\mathbf{E} - \mathrm{A} \vdots \bar{\nabla}^{*}\bar{\mathbf{H}}^{\mathrm{T}} - \bar{\rho}\mathbf{b}\,. \tag{8a}$$

In addition, RICCI's lemma on the second covariant derivative of an integrable displacement field $\mathbf{u}(\bar{\mathbf{r}}^{*}) = \mathbf{u}(\mathbf{r}^{*})$ reduces to SCHWARZ's lemma if the RIEMANN-CHRISTOFFEL-curvature tensor vanishes everywhere. Then it holds also for the jumps on an acceleration wave front. It reads

$$\bar{\mathbf{L}}^{*} = \mathbf{0}, \quad \bar{\mathbf{L}}^{*} := \left(\bar{\nabla}^{*}\mathbf{v}\right)\mathbf{E} - c\left(\bar{\nabla}^{*}\bar{\mathbf{H}}\right)\bar{\mathbf{g}}_{\bar{0}} \tag{8b}$$

and

$$\left(\bar{\nabla}^{*}\bar{\mathbf{H}}\right) : \left(\bar{\mathbf{g}}_{\bar{k}} \circ \bar{\mathbf{g}}_{\bar{l}} - \bar{\mathbf{g}}_{\bar{l}} \circ \bar{\mathbf{g}}_{\bar{k}}\right) = \mathbf{0}, \quad k,l = 1,2,3, \tag{8c}$$

on a purely spatial and a time-like manifold, respectively. Given initial fields of displacement and velocity, $\mathbf{u}_a(\bar{\mathbf{r}})$ and $\mathbf{v}_a(\bar{\mathbf{r}})$, at time $\tau = t_a$ we have the conditions

$$\mathbf{u}(\bar{\mathbf{r}}, t_a) - \mathbf{u}_a = \mathbf{0}, \quad \mathbf{v}(\bar{\mathbf{r}}, t_a) - \mathbf{v}_a = \mathbf{0}\,. \tag{8d}$$

Boundary conditions shall be given for place on the part $\partial\bar{\mathrm{B}}_v$ (points with $\bar{\mathbf{r}} = \bar{\mathbf{r}}_v$) and for traction on the part of $\partial\bar{\mathrm{B}}_\sigma$ (points with $\bar{\mathbf{r}} = \bar{\mathbf{r}}_\sigma$) of $\partial\bar{\mathrm{B}}$, $\partial\bar{\mathrm{B}} = \partial\bar{\mathrm{B}}_v \bigcup \partial\bar{\mathrm{B}}_\sigma$, $\partial\bar{\mathrm{B}}_v \bigcap \partial\bar{\mathrm{B}}_\sigma = \varnothing$.

The boundary condition of place at a point $\bar{\mathbf{r}}_v^{*} := \xi^0\bar{\mathbf{g}}_{\bar{0}} + \bar{\mathbf{r}}_v$ shall be

$$\mathbf{v}(\bar{\mathbf{r}}_v^{*}) - \mathbf{v}_b = \mathbf{0} \tag{8e}$$

with velocities $\mathbf{v}(\bar{\mathbf{r}}_v^{*})$ prescribed on $\partial\bar{\mathrm{B}}_v^{*}$ for all values of time. With a load vector $\mathbf{k}(\bar{\mathbf{r}}_\sigma^{*})$ prescribed on $\partial\bar{\mathrm{B}}_\sigma^{*}$ $(\bar{\mathbf{r}}_\sigma^{*} := \xi^0\bar{\mathbf{g}}_{\bar{0}} + \bar{\mathbf{r}}_\sigma)$ the typical boundary value condition of traction is the nonlinear equation

$$\left(\bar{\boldsymbol{\sigma}}\,\bar{\mathbf{n}}_b\right)\Big|_{\bar{\mathbf{r}}^*:=\bar{\mathbf{r}}_\sigma^*} = \mathbf{k}\left(\det\bar{\mathbf{F}}\sqrt{\bar{\mathbf{n}}_b\mathbf{C}^{-1}\bar{\mathbf{n}}_b}\right)\Big|_{\bar{\mathbf{r}}^*:=\bar{\mathbf{r}}_\sigma^*}, \tag{8f}$$

where $\bar{\mathbf{n}}_b$ is the outer normal on $\partial\bar{B}$. Eq. (8f) calls for an iterative solution, [4].

A is strongly elliptic for materials that are infinitesimally stable in HADAMARD's sense in statics. Then the boundary value problem derived from eqs. (8a, b, c, e, f) is elliptic and the initial-boundary value problem eqs. (8a - f) is hyperbolic. Therefore we apply the theory of characteristics to derive exact qualitative results and to develop numerical solution schemes.

METHOD OF CHARACTERISTICS

It is well known that systems of hyperbolic equations exhibit undetermined derivatives in certain normal directions $\bar{\mathbf{n}}^*$ in space and time. These normals define singular surfaces (so-called characteristic manifolds), on which interior derivatives are continuous, but jump discontinuities of certain exterior derivatives are admitted. The conclusive equations - the characteristic condition and the so-called compatibility equations - may be derived from the general eigenvalue problem associated with the PDE's. We make the ansatz

$$\bar{\mathbf{n}}^* := -\frac{\upsilon}{c}\bar{\mathbf{g}}_{\bar{0}} - \bar{\mathbf{n}} \tag{9}$$

for the system (8a - c) and find the characteristic condition

$$0 = \frac{1}{\bar{\rho}^2}\upsilon_0^2\det\left(\mathbf{Q}\left(\bar{\mathbf{n}}\right) - \bar{\rho}\upsilon_\varepsilon^2\left(\bar{\mathbf{n}}\right)\mathbf{E}\right), \quad \varepsilon = L, T_1, T_2 \tag{10}$$

where $\mathbf{Q}\left(\bar{\mathbf{n}}\right)$ is the acoustic tensor, defined by

$$\mathbf{Q}\left(\bar{\mathbf{n}}\right) := \left(\mathbf{g}_\lambda \circ \bar{\mathbf{n}} : \mathbf{A} : \mathbf{g}^\mu \circ \bar{\mathbf{n}}\right)\mathbf{g}^\lambda \circ \mathbf{g}_\mu . \tag{11}$$

The condition (10) may be taken as the equation for the time-like component υ of $\bar{\mathbf{n}}^*$, with an arbitrary choice of all components of the spatial normal $\bar{\mathbf{n}}$, $\bar{\mathbf{n}} \neq \mathbf{0}$.

Besides $\upsilon_0 = 0$ one obtains solutions $\upsilon_\varepsilon\left(\bar{\mathbf{n}}\right)$ of eq. (10) from the eigenvalue problem of the acoustic tensor $\mathbf{Q}$ which, in contrary to the locally isotropic wave propagation in compressible fluids, depends on the spatial direction $\bar{\mathbf{n}}$.

Therefore, for every spatial direction $\bar{\mathbf{n}}$ one has a specific eigenvalue problem. For hyperelastic materials $\mathbf{Q}\left(\bar{\mathbf{n}}\right)$ is symmetric and positive definite, and thus υ_ε^2 is positive. The eigenvectors $\mathbf{q}_\varepsilon\left(\bar{\mathbf{n}}\right)$ of $\mathbf{Q}\left(\bar{\mathbf{n}}\right)$ are real and orthogonal for any normal $\bar{\mathbf{n}}$ at a point. This situation holds even for multiple eigenvalues. $\bar{\mathbf{n}}$ and $\mathbf{q}_\varepsilon\left(\bar{\mathbf{n}}\right)$ are normalized. Then in three-dimensional space $\bar{\mathbf{n}}$ has two independent components. Furthermore, the υ_0, υ_ε are first order homogeneous functions of $\bar{\mathbf{n}}$. If one varies the components of $\bar{\mathbf{n}}$ as parameters at a material point, the vectors

$$\bar{\mathbf{n}}_0^* = \bar{\mathbf{n}}, \quad \bar{\mathbf{n}}_\varepsilon^* = -\frac{\upsilon_\varepsilon}{c}\bar{\mathbf{g}}_{\bar{0}} + \bar{\mathbf{n}} \tag{12}$$

generate the normal hypercones N_0^*, N_ε^*. The according local characteristic hyperplanes envelope the local MONGE-hypercones M_0^*, M_ε^*. The lines of tangency are given by the bicharacteristics $\bar{\mathbf{m}}_0^*$, $\bar{\mathbf{m}}_\varepsilon^*$ (generators of M_0^*, M_ε^*). The local characteristic hyperplanes represent plane wave fronts and the MONGE-hypercones represent the wave fronts emanating from a point disturbance at their apex. For two space dimensions and time the situation is demonstrated in Fig. 1. It shows typical calculated wave fronts emanating from point P_9 in an isotropic plate under pure stretch.

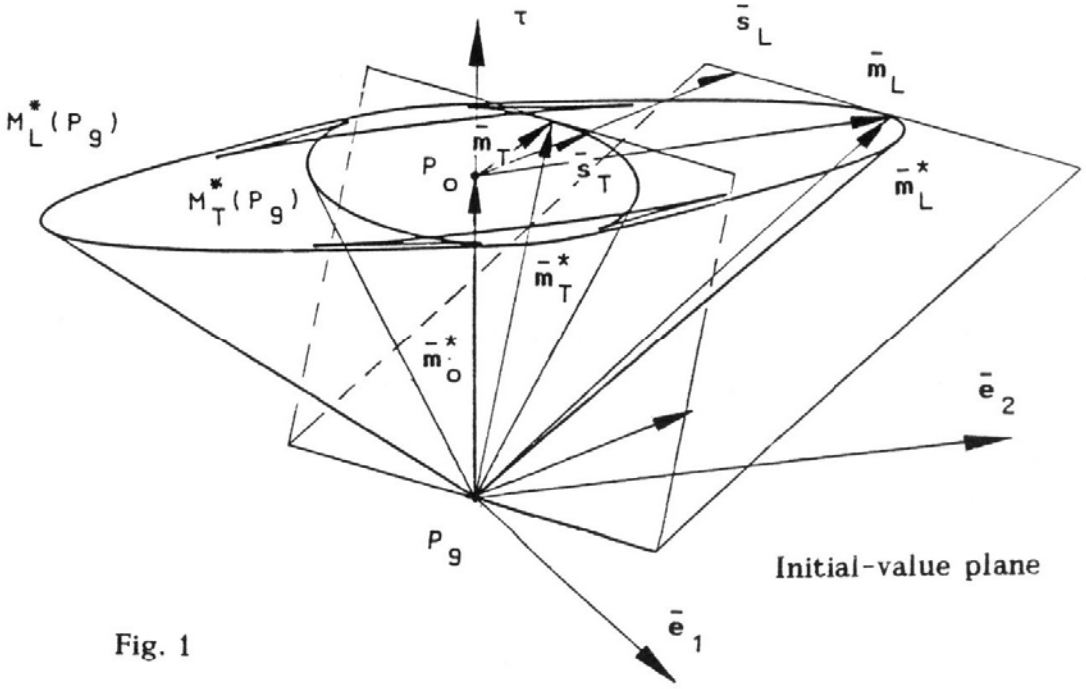

Fig. 1

The normal $\bar{\mathbf{n}}_0^*$ is purely spatial and thus defines a material singular surface. Crossing it the lowest order discontinuous derivative is purely spatial. The according MONGE-cone degenerates to the particle path line. The normals $\bar{\mathbf{n}}_\varepsilon^*$, define acceleration waves with possibly discontinuous time-like derivatives $\left(\bar{\nabla}^*\bar{\mathbf{H}}\right)\bar{\mathbf{n}}_\varepsilon^*$, $\left(\bar{\nabla}^*\mathbf{v}\right)\bar{\mathbf{n}}_\varepsilon^*$. From the orthogonality of the eigenvectors $\mathbf{q}_\varepsilon(\bar{\mathbf{n}})$ one deduces that the jumps on different MONGE-hypercones through a point are orthogonal to each other. But these waves are purely longitudinal and transversal only on the axis of symmetry of the cones, because only there $\mathbf{q}(\bar{\mathbf{n}})$ is parallel to $\bar{\mathbf{n}}$. These axes are called acoustical axes and waves propagating in these directions are called principal waves. In a deformed isotropic elastic material the eigenvectors of $\bar{\bar{\boldsymbol{\sigma}}}$ and $\mathbf{C}$ or $\mathbf{G}$ are collinear with the acoustical axes $\bar{\mathbf{e}}$. Transformation into the actual configuration is via $\mathbf{e} = \bar{\mathbf{F}}\bar{\mathbf{e}}\left|\bar{\mathbf{F}}\bar{\mathbf{e}}\right|^{-1}$. If some initial amplitude of the jump discontinuity is known, its future magnitude can be calculated from the transport equation, [7].

Definition (11) allows $\mathbf{A}$ to be written in terms of principle wave speeds, which can be found from ultrasound wave speed measurements. Unfortunately, not all components may be measured from sound disturbances superimposed on the standard uniaxial tension test. There are two principal axes $\bar{\mathbf{e}}_1$, $\bar{\mathbf{e}}_2$ in two-dimensional stress given by eqs. (4c, d). Taking care of $\upsilon_T(\bar{\mathbf{e}}_1) = \upsilon_T(\bar{\mathbf{e}}_2) =: \upsilon_T$ we have

$$\begin{aligned}\frac{1}{\bar{\rho}}\mathbf{A} := \quad & \upsilon_L^2(\bar{\mathbf{e}}_1)\mathbf{e}_1 \circ \bar{\mathbf{e}}_1 \circ \mathbf{e}_1 \circ \bar{\mathbf{e}}_1 + \upsilon_L^2(\bar{\mathbf{e}}_2)\mathbf{e}_2 \circ \bar{\mathbf{e}}_2 \circ \mathbf{e}_2 \circ \bar{\mathbf{e}}_2 \\ & + \upsilon_T^2(\mathbf{e}_2 \circ \bar{\mathbf{e}}_1 \circ \mathbf{e}_2 \circ \bar{\mathbf{e}}_1 + \mathbf{e}_1 \circ \bar{\mathbf{e}}_2 \circ \mathbf{e}_1 \circ \bar{\mathbf{e}}_2) \\ & + \kappa^2(\mathbf{e}_1 \circ \bar{\mathbf{e}}_1 \circ \mathbf{e}_2 \circ \bar{\mathbf{e}}_2 + \mathbf{e}_1 \circ \bar{\mathbf{e}}_1 \circ \mathbf{e}_2 \circ \bar{\mathbf{e}}_2)\ .\end{aligned} \tag{13}$$

In three-dimensional stress fields the values of υ_T are different in different principal directions generally. The component κ^2 can neither be interpreted as wave speed nor be calculated from wave speeds (except for special constitutive equations such as for linear isotropic elastic material in small deformation theory). Both local effects, the difference $\upsilon_L(\bar{\mathbf{e}}_1) - \upsilon_L(\bar{\mathbf{e}}_2)$ and the rotation of $\bar{\mathbf{e}}$ have been used for a pointwise measurement of stress fields [8]. A small point disturbance in a deformed istropic elastic body will only propagate on spherical wave fronts if the underlying stress is hydrostatic (or the body is made from a material with a special form of the constitutive equation).

The anisotropy of the local wave propagation depending on the local deformation may lead to self-intersections of the quasi-transversal MONGE-cones and to crunodes and cusps with local focussing on their conics. These phenomena result in gaps which were called lacunae by PETROWSKY [9] and lie like islands in the domain of dependence. For linear anisotropic media, various criteria for the existence of lacunae behind the wave fronts of point disturbances have been found [1, 4, 9, 10]. But no direct results are known for the nonlinear case except by arguments for the locally linearized equations [11]. Further information on anisotropic wave propagation in solids may be found in [12] for linear elastic deformation and in [13] for compressible plastic deformation.

There are infinitely many ways to describe the propagation of a plane wave. We use the bicharacteristics $\mathbf{m}_0^*$ and $\mathbf{m}_\varepsilon^*$ with the rays $\bar{\mathbf{m}}_\varepsilon$ in space,

$$\bar{\mathbf{m}}_0^* := c\bar{\mathbf{g}}_{\bar{0}}\,, \tag{14a}$$

$$\bar{\mathbf{m}}_\varepsilon^* := \bar{\mathbf{m}}_0^* + \bar{\mathbf{m}}_\varepsilon = \bar{\mathbf{m}}_0^* + \frac{\partial \upsilon_\varepsilon}{\partial \bar{\mathbf{n}}} = \bar{\mathbf{m}}_0^* + \bar{\mathbf{m}}_\varepsilon \frac{1}{2\bar{\rho}\upsilon_\varepsilon}\mathbf{q}_\varepsilon \circ \mathbf{q}_\varepsilon : \frac{\partial \mathbf{Q}}{\partial \bar{\mathbf{n}}}\,, \tag{14b}$$

and the nearcharacteristics $\bar{\mathbf{s}}_\varepsilon^*$ with the normal velocity $\bar{\mathbf{s}}_\varepsilon$,

$$\bar{\mathbf{s}}_\varepsilon^* := \bar{\mathbf{m}}_0^* + \bar{\mathbf{s}}_\varepsilon = \bar{\mathbf{m}}_0^* + \upsilon_\varepsilon \bar{\mathbf{n}} = \bar{\mathbf{m}}_0^* + \bar{\mathbf{m}}_\varepsilon \frac{1}{\bar{\rho}\upsilon_\varepsilon}\mathbf{q}_\varepsilon \circ \mathbf{q}_\varepsilon : \mathbf{Q} \circ \bar{\mathbf{n}}.\,, \tag{15}$$

Any other time-like vector in the characteristic hyperplane tangent to the MONGE cone M_ε^* is also called near-characteristic, but will not be needed here. For plane problems the space-like tangent $\mathbf{t}$ and either $\bar{\mathbf{m}}_\varepsilon^*$ or $\bar{\mathbf{s}}_\varepsilon^*$ span the characteristic surface elements. By the vectors $\bar{\mathbf{m}}_\varepsilon^*$ and $\bar{\mathbf{s}}_\varepsilon^*$ two total time derivatives in a characteristic hyperplane can be introduced,

$$\left(\bar{\nabla}^* f\right)\bar{\mathbf{m}}_\varepsilon^* := \frac{\partial f}{\partial \tau} + \left(\bar{\nabla} f\right)\bar{\mathbf{m}} \tag{16a}$$

and the so-called δ-time derivative

$$\left(\bar{\nabla}^* f\right)\bar{\mathbf{s}}_\varepsilon^* := \frac{\partial f}{\partial \tau} + \left(\bar{\nabla} f\right)\bar{\mathbf{s}}, \tag{16b}$$

also known as displacement derivative. The discussion was only local so far. In finite time a point disturbance propagates along MONGE-conoids which may be twisted. For the integration of some function f on M_ε one may use the canonical HAMILTON equations for the HAMILTONIan υ_ε. With $\bar{\mathbf{n}}$ normalized and υ_ε as a function of $\bar{\mathbf{n}}$, $\bar{\mathbf{r}}$, τ we derive the special form of the HAMILTON equations

$$\left(\bar{\nabla}^* \bar{\mathbf{n}}\right)\bar{\mathbf{m}}_\varepsilon^* = \left(\bar{\mathbf{n}} \circ \bar{\mathbf{n}} - \mathbf{E}\right)\bar{\nabla}\upsilon_\varepsilon, \tag{17a}$$

$$\left(\bar{\nabla}^* \bar{\mathbf{r}}\right)\bar{\mathbf{m}}_\varepsilon^* = \frac{\partial \upsilon_\varepsilon}{\partial \bar{\mathbf{n}}}. \tag{17b}$$

Different proofs of these equations were given in [4, 14]. Instead of eqs. (17a, b), we get for $\bar{\mathbf{s}}_\varepsilon^*$

$$\left(\bar{\nabla}^* \bar{\mathbf{n}}\right)\bar{\mathbf{s}}_\varepsilon^* = \left(\bar{\mathbf{n}} \circ \bar{\mathbf{n}} - \mathbf{E}\right)\bar{\nabla}\upsilon_\varepsilon, \tag{18a}$$

$$\left(\bar{\nabla}^* \bar{\mathbf{r}}\right)\bar{\mathbf{s}}_\varepsilon^* = \upsilon_\varepsilon \bar{\mathbf{n}}. \tag{18b}$$

Different proofs of the famous HAYES-THOMAS-formula (18a) may be found in [4, 15, 16, 17, 18]. It is assumed that the equation of the wave surface in space and time has continuous second derivatives in space. Thus eqs. (17a), (18a) do not hold on cusps. In [4] it is shown that no torsion of the wave front occurs in plane problems.

The purpose of the discussion of point disturbances is to replace the initial set of PDE's (8a, b) by a linearly independent set of so-called compatibility equations in which no undetermined derivatives appear. These equations only hold in characteristic surfaces. On M_0^* one gets for $\bar{\mathbf{n}}_0^* = \bar{\mathbf{n}}$

$$\mathbf{0} = \bar{\mathbf{L}}^* \bar{\mathbf{t}}, \tag{19a}$$

and on M_ε^* for $\bar{\mathbf{n}}_\varepsilon^*$

$$0 = \mathbf{q}_\varepsilon\left(\bar{\mathbf{n}}\right)\left(\upsilon_\varepsilon\left(\bar{\mathbf{n}}\right)\mathbf{l} - \mathbf{A} : \left(\bar{\mathbf{n}} \circ \bar{\mathbf{L}}^*\right)\right). \tag{19b}$$

In a more extended notation for plane problems,

$$\mathbf{0} = \left(\bar{\nabla}^* \bar{\mathbf{H}}\right) : \bar{\mathbf{t}} \circ \bar{\mathbf{m}}_0^* - \left(\bar{\nabla}^* \mathbf{v}\right) \bar{\mathbf{t}} \,, \tag{20a}$$

$$\begin{aligned} 0 = & \left(\bar{\rho} \upsilon_\varepsilon \mathbf{q}_\varepsilon \circ \bar{\mathbf{m}}_\varepsilon^* + \mathbf{q}_\varepsilon \circ \bar{\mathbf{n}} : \mathbf{A} \bar{\mathbf{t}} \circ \bar{\mathbf{t}} - \bar{\rho} \upsilon_\varepsilon \left(\bar{\mathbf{m}}_\varepsilon \bar{\mathbf{t}}\right) \mathbf{q}_\varepsilon \circ \bar{\mathbf{t}}\right) : \bar{\nabla}^* \mathbf{v} \\ & - \left(\mathbf{q}_\varepsilon \circ \bar{\mathbf{n}} : \mathbf{A} \circ \bar{\mathbf{m}}_\varepsilon^* + \upsilon_\varepsilon \mathbf{q}_\varepsilon \circ \bar{\mathbf{t}} : \mathbf{A} \circ \bar{\mathbf{t}} - \left(\bar{\mathbf{m}}_\varepsilon \bar{\mathbf{t}}\right) \mathbf{q}_\varepsilon \circ \bar{\mathbf{n}} : \mathbf{A} \circ \bar{\mathbf{t}}\right) : \bar{\nabla}^* \bar{\mathbf{H}} \\ & - \bar{\rho} \upsilon_\varepsilon \mathbf{q}_\varepsilon \mathbf{b} \,, \end{aligned} \tag{20b}$$

one can see that only interior derivatives remain. These are the cross derivatives in direction of $\bar{\mathbf{t}}$ and the derivatives in characteristic directions $\bar{\mathbf{m}}_\varepsilon^*$ which may be replaced by $\bar{\mathbf{s}}_\varepsilon^*$ in a near-characteristics method. Using $\bar{\mathbf{s}}_\varepsilon \bar{\mathbf{t}} = 0$ eq. (20b) becomes

$$\begin{aligned} 0 = & \left(\bar{\rho} \upsilon_\varepsilon \mathbf{q}_\varepsilon \circ \bar{\mathbf{s}}_\varepsilon^* + \mathbf{q}_\varepsilon \circ \bar{\mathbf{n}} : \mathbf{A} \bar{\mathbf{t}} \circ \bar{\mathbf{t}}\right) : \bar{\nabla}^* \mathbf{v} \\ & - \left(\mathbf{q}_\varepsilon \circ \bar{\mathbf{n}} : \mathbf{A} \circ \bar{\mathbf{s}}_\varepsilon^* + \upsilon_\varepsilon \mathbf{q}_\varepsilon \circ \bar{\mathbf{t}} : \mathbf{A} \circ \bar{\mathbf{t}}\right) : \bar{\nabla}^* \bar{\mathbf{H}} - \bar{\rho} \upsilon_\varepsilon \mathbf{q}_\varepsilon \mathbf{b} \,. \end{aligned} \tag{20c}$$

To this end all equations are exact and hold for arbitrary large deformation and large displacement of a general isotropic nonlinear hyperelastic body. The assumption of the existence of a stored energy density was a mere simplification of notation. Its only effect is the symmetry imposed upon $\mathbf{A}$ by eq. (7b).

NUMERICAL SOLUTION

Given the initial data at points of a suitable mesh on the initial value plane at time $\tau = t_a$, the solution at a point P_0 on the plane $\tau = t_0 + \Delta\tau$ may be computed numerically by integrating the HAMILTON equations (17a, b) and the compatibility equations, which are given for the plane problem by equations (20a, b). We actually integrate the simplified equations (18a, b) and (20a, c). From Fig. 1 it is clear that a near-characteristics method uses points outside the analytical domain of dependence. Therefore, we integrate in characteristic hypersurfaces which are principal waves at point P_0. For principal waves, the two integration paths are equivalent In the limit $\Delta\tau \to 0$, since $\bar{\mathbf{m}}_\varepsilon^* = \bar{\mathbf{s}}_\varepsilon^*$. The principal axes at P_0 depend on the iterative solution. Therefore, we have to rotate the local basis in each iteration step. This expense is compensated by the condensed presentation (13) of $\mathbf{A}$. In the initial value surface all functions and the cross derivatives may be calculated from a constrained least squares approximation with constraints following from eq. (8c). If the cross derivatives at P_0 are considered as additional unknowns, eqs. (18a,b), (20a,c) contain only total time derivatives in directions $\bar{\mathbf{s}}_0^*$ and $\bar{\mathbf{s}}_\varepsilon^*$. These ODE's may be integrated by HEUN's second order method. It can be shown that the number of linearly independent difference equations derived from eqs. (20a,c) is less than the number of unknown functions including the cross derivatives at P_0 Therefore, we integrate the non characteristic balance of momentum (8a) along the path line to get two additional equations. This was suggested for problems of linear elasto-

dynamics in [19] and for gas dynamics in [20]. On the path line all derivatives in (8a) are continuous because it is a material singular surface. Fig. 2 shows the scheme we use for an interior point of the plate. The numbers of the points in the scheme correspond to the indices written in the difference equations. Fig. 1 and Fig. 2 indicate that the CFL stability condition is satisfied. Note that the iteration may be started with the first order EULER-CAUCHY-integration of (8b) along the path line to give $\bar{\mathbf{H}}_0$ at P_0, since a first guess of $\mathbf{v}_0$ is not needed in elastodynamics. The algorithm may be read from Fig. 2 and the following formulas:

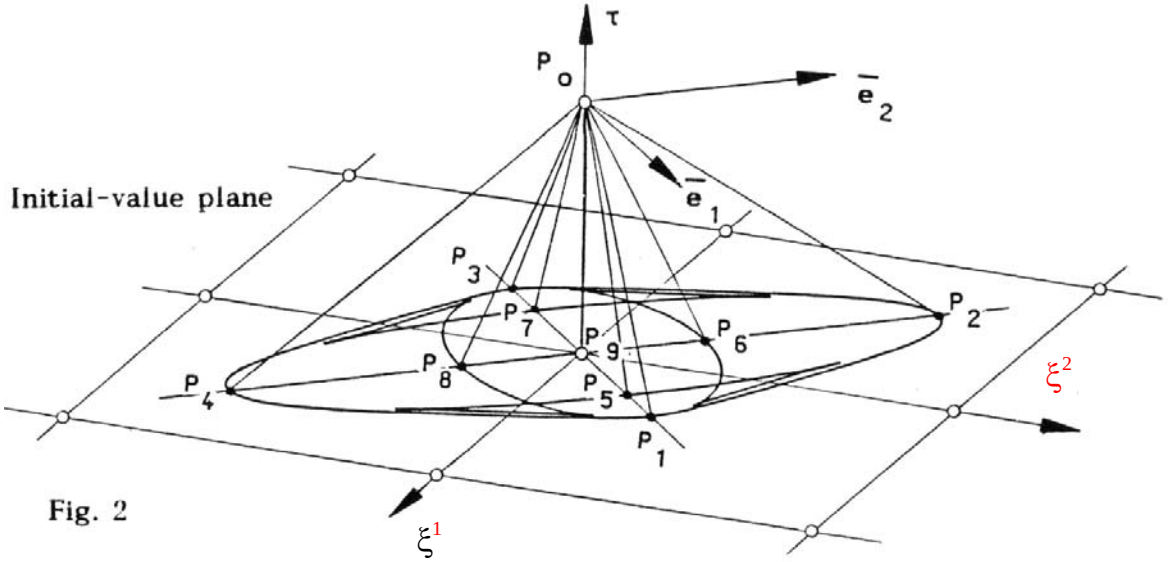

Fig. 2

Praedictor (first guess): $i = 1(1)9$ with $\upsilon_0 = 0$ for $i = 9$

$$\bar{\mathbf{r}}_i^{*(0)} = \bar{\mathbf{r}}_9^{*} + \Delta\tau\left[\bar{\mathbf{e}}\upsilon_{\varepsilon 0}\left(\bar{\mathbf{e}}\right)\right]^{(0)}, \tag{21a}$$

and from the compatibility equation along the path line

$$\bar{\mathbf{H}}_0^{(0)} = \bar{\mathbf{H}}_9 + \Delta\tau\bar{\nabla}\mathbf{v}_9\,. \tag{22a}$$

Corrector (k -th iteration step):

$$\bar{\mathbf{r}}_i^{*(k)} = \bar{\mathbf{r}}_9^{*} + \frac{\Delta\tau}{2}\left[\bar{\mathbf{e}}\left(\upsilon_{\varepsilon i}\left(\bar{\mathbf{e}}\right) + \upsilon_{\varepsilon 0}\left(\bar{\mathbf{e}}\right)\right)\right]^{(k-1)}, \tag{21b}$$

$$\bar{\mathbf{H}}_0^{(k)} = \bar{\mathbf{H}}_9 + \frac{\Delta\tau}{2}\left[\bar{\nabla}\mathbf{v}_9 + \bar{\nabla}\mathbf{v}_0^{(k-1)}\right]. \tag{22b}$$

We derive the difference equations for principal waves arriving at point P_0 (see Fig. 2) from the compatibility equations on the quasi-longitudinal cone M_L^* and the quasi-transversal cone M_T^*. The appropriate choices of $\bar{\mathbf{n}}_{0i}$ $(i=1(1)4)$ and $\bar{\mathbf{n}}_{0j}$ $(j=5(1)8)$ are $\bar{\mathbf{e}}_1$, $\bar{\mathbf{e}}_2$, $-\bar{\mathbf{e}}_1$, $-\bar{\mathbf{e}}_2$. We give an example of the difference equations on each cone.

From the compatibility equation on the quasi-longitudinal cone M_L^* with $\bar{\mathbf{n}}_{0i} := \bar{\mathbf{e}}_1$ and $\bar{\mathbf{t}}_{0i} := \bar{\mathbf{e}}_2$ and $\mathbf{q}_{Li} = \mathbf{q}_{Li}(\bar{\mathbf{e}}_1)$ for $i=1$ it follows:

$$
\begin{aligned}
&\left[\upsilon_{L0}(\bar{\mathbf{e}}_1)\mathbf{e}_1 + \upsilon_{Li}(\bar{\mathbf{e}}_1)\mathbf{q}_{Li}\right]^{(k-1)} \mathbf{v}_0^{(k)} \\
&-\left[\upsilon_{L0}^2(\bar{\mathbf{e}}_1)\mathbf{e}_1 \circ \bar{\mathbf{e}}_1 + \kappa_0^2 \mathbf{e}_2 \circ \bar{\mathbf{e}}_2 + \frac{1}{\bar{\rho}}\upsilon_{Li}(\bar{\mathbf{e}}_1)\mathbf{q}_{Li} \circ \bar{\mathbf{e}}_1 : \mathbf{A}_i\right]^{(k-1)} : \bar{\mathbf{H}}_0^{(k)} \\
&-\Delta\tau\Big[-\left(\kappa_0^2 \mathbf{e}_2 \circ \bar{\mathbf{e}}_2\right)^{(k-1)} : \bar{\nabla}\mathbf{v}_0^{(k)} \\
&+\left(\upsilon_{L0}(\bar{\mathbf{e}}_1)\left(\upsilon_{T0}^2 \mathbf{e}_1 \circ \bar{\mathbf{e}}_2 \circ \bar{\mathbf{e}}_2 + \kappa_0^2 \mathbf{e}_2 \circ \bar{\mathbf{e}}_1 \circ \bar{\mathbf{e}}_2\right)\right)^{(k-1)} : \bar{\nabla}\bar{\mathbf{H}}_0^{(k)} \\
&+\left(\upsilon_{L0}(\bar{\mathbf{e}}_1)\mathbf{e}_1\mathbf{b}_0\right)^{(k-1)}\Big] \\
&=\Big\{\left[\upsilon_{L0}(\bar{\mathbf{e}}_1)\mathbf{e}_1 + \upsilon_{Li}(\bar{\mathbf{e}}_1)\mathbf{q}_{Li}\right]\mathbf{v}_i \\
&\quad -\left[\upsilon_{L0}^2(\bar{\mathbf{e}}_1)\mathbf{e}_1 \circ \bar{\mathbf{e}}_1 + \kappa_0^2 \mathbf{e}_2 \circ \bar{\mathbf{e}}_2 + \frac{1}{\bar{\rho}}\upsilon_{Li}(\bar{\mathbf{e}}_1)\mathbf{q}_{Li} \circ \bar{\mathbf{e}}_1 : \mathbf{A}_i\right] : \bar{\mathbf{H}}_i \\
&\quad -\Delta\tau\Big[\frac{1}{\bar{\rho}}\mathbf{q}_{Li} \circ \bar{\mathbf{e}}_1 : \mathbf{A}_i \bar{\mathbf{e}}_2 \circ \bar{\mathbf{e}}_2 : \bar{\nabla}\mathbf{v}_i \\
&\quad +\frac{1}{\bar{\rho}}\upsilon_{Li}(\bar{\mathbf{e}}_1)\mathbf{q}_{Li} \circ \bar{\mathbf{e}}_2 : \mathbf{A}_i \circ \bar{\mathbf{e}}_2 : \bar{\nabla}\bar{\mathbf{H}}_i + \upsilon_{Li}(\bar{\mathbf{e}}_1)\mathbf{q}_{Li}\mathbf{b}_0\Big\}^{(k-1)}.
\end{aligned}
\tag{23}
$$

From the compatibility equation on the quasi-transversal cone M_T^* with $\bar{\mathbf{n}}_{0j} := \bar{\mathbf{e}}_1$ and $\bar{\mathbf{t}}_{0j} := \bar{\mathbf{e}}_2$ and $\mathbf{q}_{Tj} = \mathbf{q}_{Tj}(\bar{\mathbf{e}}_1)$ for $j=5$ it follows:

$$
\begin{aligned}
&\left[\upsilon_{T0}\mathbf{e}_2 + \upsilon_{Ti}\mathbf{q}_{Li}\right]^{(k-1)} \mathbf{v}_0^{(k)} \\
&-\left[\upsilon_{T0}^2 \mathbf{e}_2 \circ \bar{\mathbf{e}}_1 + \kappa_0^2 \mathbf{e}_1 \circ \bar{\mathbf{e}}_2 + \frac{1}{\bar{\rho}}\upsilon_{Ti}\mathbf{q}_{Li} \circ \bar{\mathbf{e}}_1 : \mathbf{A}_i\right]^{(k-1)} : \bar{\mathbf{H}}_0^{(k)} \\
&-\Delta\tau\Big[-\left(\kappa_0^2 \mathbf{e}_1 \circ \bar{\mathbf{e}}_2\right)^{(k-1)} : \bar{\nabla}\mathbf{v}_0^{(k)} \\
&+\left(\upsilon_{T0}\left(\upsilon_{L0}^2(\bar{\mathbf{e}}_2)\mathbf{e}_2 \circ \bar{\mathbf{e}}_2 \circ \bar{\mathbf{e}}_2 + \kappa_0^2 \mathbf{e}_1 \circ \bar{\mathbf{e}}_1 \circ \bar{\mathbf{e}}_2\right)\right)^{(k-1)} : \bar{\nabla}\bar{\mathbf{H}}_0^{(k)} \\
&+\left(\upsilon_{T0}\mathbf{e}_2\mathbf{b}_0\right)^{(k-1)}\Big] \\
&=\Big\{\left[\upsilon_{T0}\mathbf{e}_2 + \upsilon_{Ti}\mathbf{q}_{Ti}\right]\mathbf{v}_i \\
&\quad -\left[\upsilon_{T0}^2 \mathbf{e}_2 \circ \bar{\mathbf{e}}_1 + \kappa_0^2 \mathbf{e}_1 \circ \bar{\mathbf{e}}_2 + \frac{1}{\bar{\rho}}\upsilon_{Ti}\mathbf{q}_{Ti} \circ \bar{\mathbf{e}}_1 : \mathbf{A}_i\right] : \bar{\mathbf{H}}_i \\
&\quad -\Delta\tau\Big[\frac{1}{\bar{\rho}}\mathbf{q}_{Ti} \circ \bar{\mathbf{e}}_1 : \mathbf{A}_i \bar{\mathbf{e}}_2 \circ \bar{\mathbf{e}}_2 : \bar{\nabla}\mathbf{v}_i \\
&\quad +\frac{1}{\bar{\rho}}\upsilon_{Ti}\mathbf{q}_{Ti} \circ \bar{\mathbf{e}}_2 : \mathbf{A}_i \circ \bar{\mathbf{e}}_2 : \bar{\nabla}\bar{\mathbf{H}}_i + \upsilon_{Ti}\mathbf{q}_{Ti}\mathbf{b}_0\Big\}^{(k-1)}.
\end{aligned}
\tag{24}
$$

We complete the difference equations with the balance of momentum

$$\mathbf{v}_0^{(k)} - \frac{\Delta\tau}{2}\left[\left(\frac{1}{\bar{\rho}}\mathbf{A}_0\right)^{(k-1)} : \left(\bar{\nabla}\bar{\mathbf{H}}_0^{T}\right)^{(k)} + \mathbf{b}_0\right] = \mathbf{v}_9 + \frac{\Delta\tau}{2}\left(\frac{1}{\bar{\rho}}\mathbf{A}_9 : \bar{\nabla}\bar{\mathbf{H}}_9^{T} + \mathbf{b}_9\right). \tag{25}$$

If we are not interested in the gradients at P_0 we may eliminate them by linear combinations of the difference equations and just calculate $\mathbf{v}_0$ and $\bar{\mathbf{H}}_0$. After the solutions at all points at time $\tau = t_a + \Delta\tau$ are calculated they may be used as initial data for the following time step.

On boundaries some difference equations are not needed. But only in linear problems they may be replaced by boundary values. The schemes for the nonlinear problem use the approximation of $\bar{\nabla}\bar{\mathbf{H}}_0$ at P_0, [4]. They also need some iteration to solve (8f). The only reason for both disadvantages is the nonlinearity of the boundary condition (8f).

NUMERICAL EXAMPLES

Fig. 3a shows the simple elongation strain path of a typical rubber-like material using TRELOAR's approximation with data from [21]. The functions ψ_0' and ψ_1' in eq. (4b) are approximated by second degree polynomials in the eigenvalues of $\mathbf{C}$. Up to point 3 lower degree polynomials would result in roughly the same curve since the geometrical nonlinearity is predominant. But this is not the case for the wave speeds [4]. Obviously only $\upsilon_L(\bar{\mathbf{e}}_1)$ can he deduced from the uniaxial stress-strain curve. Fig. 3b represents the related principal wave speeds. For three different homogeneous states of stresses (uniaxial pressure (1), no stresses (2), uniaxial tension (3)). Fig. 3c shows typical wave fronts of infinitesimal point disturbances in a plate, i.e. lines of intersection of the MONGE-cones with a space-like plane. The state (3) was used for a numerical test, where a small shear deformation was superimposed by an initial disturbance of the velocity component $\mathbf{ve}_2$. Both of the MONGE-cones come out nicely and the two wave types seem decoupled. The amplitudes of $\mathbf{ve}_2$ are approximately ten times higher than those of $\mathbf{ve}_1$. In another example, for a plate made of a compressible material, we found a strong coupling of the two types of waves [4].

Since at the state 1 $\upsilon_L(\bar{\mathbf{e}}_1)$ increases steeply with growing pressure one expects pressure waves to form shocks quickly. The initial profile of the wave in Fig. 4 changes in the predicted way while moving to the right. Clearly, there is also an equalisation in the transverse direction.

ACKNOWLEDGEMENT

The present investigation was financially supported by the Deutsche Forschungs-gemeinschaft.

REFERENCES

[1] PAYTON, R.G.: Elastic Wave Propagation in Transversely Isotropic Media. Martinus Nijhoff, The Hague (1983).

[2] JEFFREY, A.; TANIUTI, T.: Non-Linear Wave Propagation with Applications to Physics and Magnetohydrodynamics. Academic Press, New York (1964).

[3] BALLMANN, J.; RAATSCHEN, H.J.; STAAT, M.: High Stress Intensities in Focussing Zones of Waves. In P. LADEVESE (Ed.): Local Effects in the Analysis of Structures. Elsevier, Amsterdam (1985).

[4] STAAT, M.: Nichtlineare Wellen in elastischen Scheiben. Dr.-Ing. Thesis, RWTH-Aachen (1987).

[5] KRAWIETZ, A.: Materialtheorie, Springer, Berlin (1986).

[6] STAAT, M.; BALLMANN, J.: Zur Problematik tensorieller Verallgemeinerungen einachsiger nichtlinearer Materialgesetze. ZAMM, 69 (1989) 73-81.

[7] BRAUN, M.: Wave Propagation in Elastic Membranes. In U. NIGUL, J. ENGELBRECHT (Ed.): Nonlinear Deformation Waves. Springer, Berlin (1983).

[8] PAO, Y.-H.; SACHSE, W.; FUKUOA, H.: Acoustoelasticity and Ultrasonic Measurements of Residual Stresses. Physical Acoustics 17, Academic Press, New York (1984) Chap. 2.

[9] PETROWSKY, I.G.: On the Diffusion of Waves and the Lacunas for Hyperbolic Equations. Rec. Math. (Math. Sbornic) 17 (1945) 289-370.

[10] BURRIDGE, R.: Lacunas in Two-Dimensional Wave Propagation. Proc. Camb. Phil. Soc. 63 (1967) 819-825.

[11] PAYTON, R.G.: Two Dimensional Wave Front Shape Induced in a Homogeneously Strained Elastic Body by a Point Perturbing Body Force. Arch. Rat. Mech. 32 (1969) 311-330 and 35 (1969) 402-408.

[12] MUSGRAVE, M.J.P.: Crystal Acoustics. Holden-Day, San Francisco (1970).

[13] SAUERWEIN, H.: Anisotropic Waves in Elastoplastic Soils. Int. J. Engng. Sci. 5 (1967) 455-475.

[14] VARLEY, E.; CUMBERBATCH, E.: Non-linear Theory of Wave-front Propagation. J. Inst. Maths. Applics. 1 (1965) 101-112.

[15] ERINGEN, A.C.; SUHUBI, E.S.: Elastodynamics I, Academic Press, New York (1974).

[16] THOMAS, T.Y.: Plastic Flow and Fracture in Solids. Academic Press, New York (1961).

[17] TRUESDELL, C.; TOUPIN, R.A.: The Classical Field Theories. In S. FLÜGGE (Ed.): Handbuch der Physik III/I. Springer, Berlin (1960).

[18] WANG, C.C.; TRUESDELL, C.: Introduction to Rational Elasticity. Nordhoff, Leyden (1973).

[19] CLIFTON, R.J.: A Difference Method for Plane Problems In Dynamic Elasticity. Quart. of Appl. Math. 25 (1967) 97-116.

[20] BUTLER, D.S.: The Numerical Solution of Hyperbolic Systems of Partial Differential Equations in Three Independent Variables. Proc. Roy. Soc., A 255 (1966) 232-252.

[21] HAINES, D.W.; WILSON, W.D.: Strain-Energy Density Function for Rubber-like Materials, J. Mech. Phys. Solids 27 (1979) 331-343.

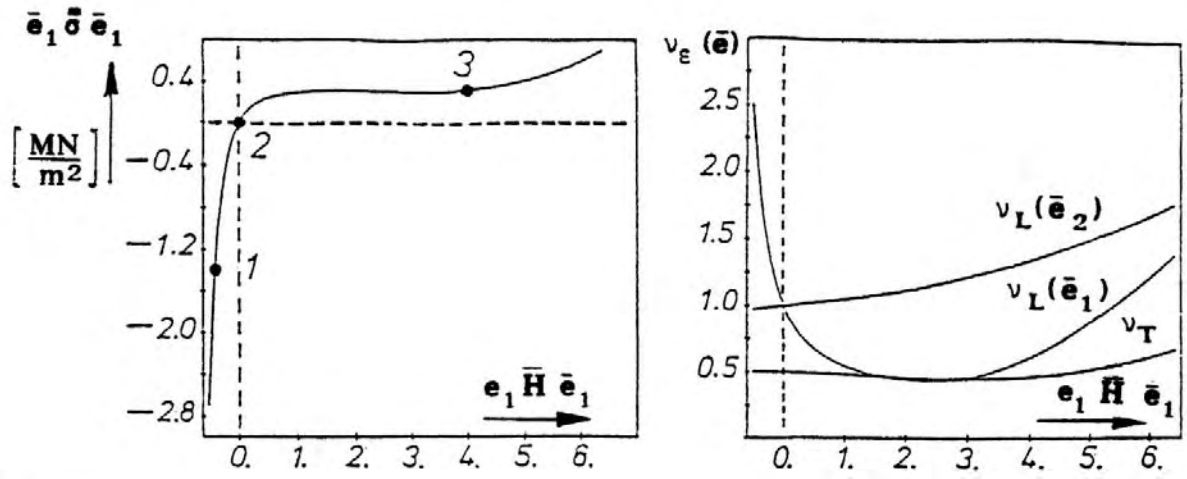

Fig. 3a

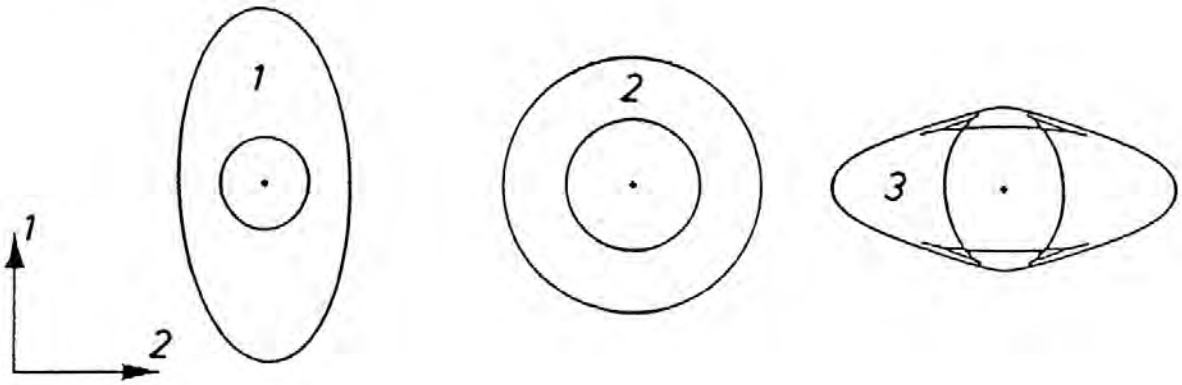

Fig. 3b

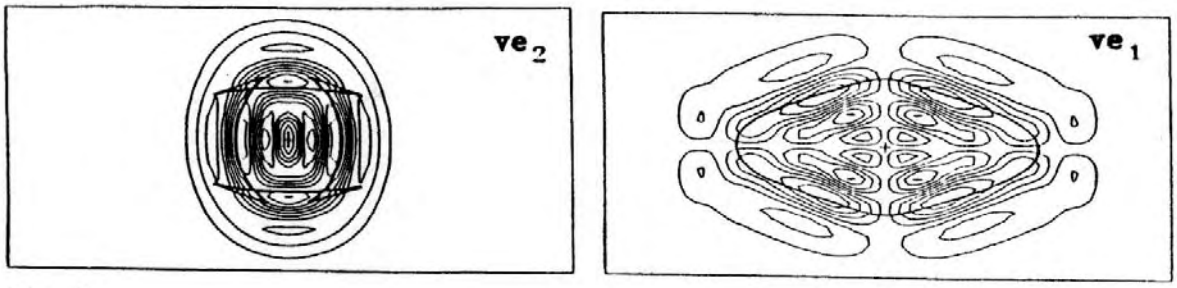

Fig. 3c

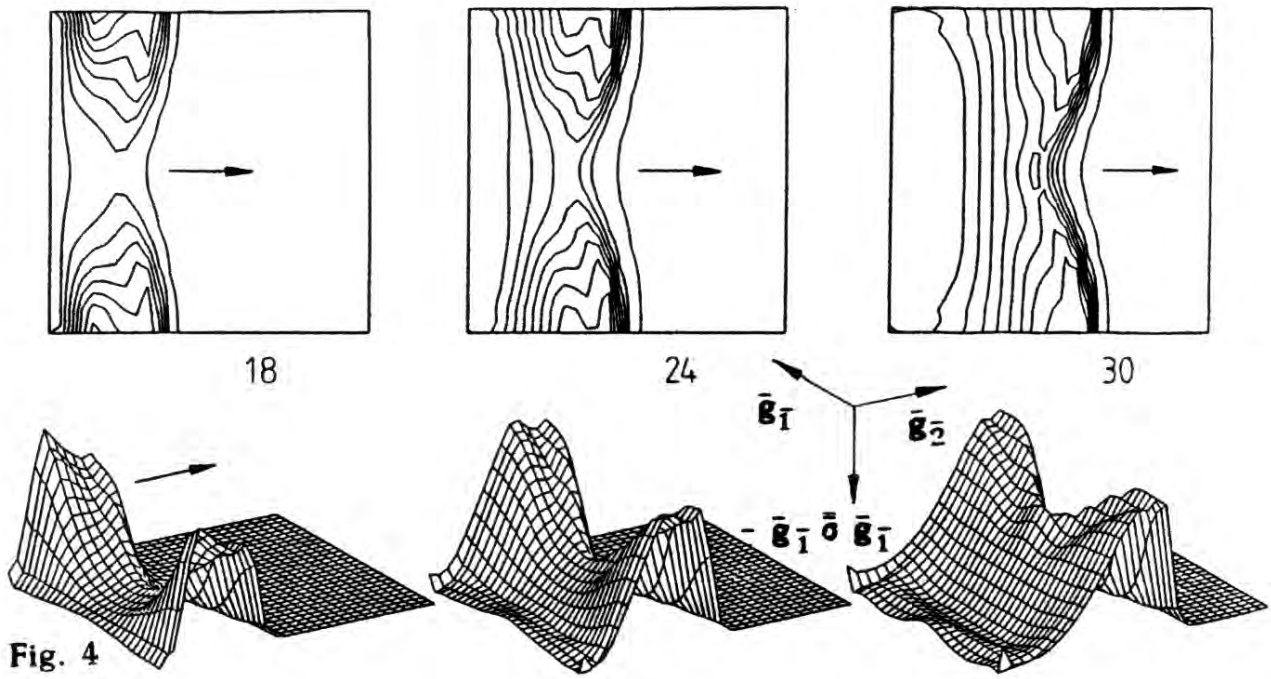

Fig. 4